JOURNAL OF MATERIALS SCIENCE 33 (1998) 139–145

Interaction of some pollutant oxides on durability of silicon carbide as a material for diesel vehicle filters

M. T. DARIO, A. BACHIORRINI
Dipartimento di Scienze e Technologie Chimiche, Università di Udine, Via del Cotonificio 108, 33100 Udine, Italy

The short-term interaction of SiC and some single pollutant oxides (Na_2O, PbO and V_2O_5) was investigated as a function of temperature by X-ray diffraction (XRD) and Fourier transform infrared (F.T–i.r.) analysis. Sodium oxide dissolves the protective silica layer forming glassy sodium silicates at a temperature of 550 °C. V_2O_5 accelerates SiC oxidation, leading to the formation of large amounts of silica at temperatures above 750 °C. PbO begins to react with silica film at 600 °C forming Pb_2SiO_4. Degradation becomes highly destructive at higher temperatures. Given the presence of Na_2O, PbO and V_2O_5 in diesel particulates and the temperatures that filters must tolerate, SiC appears to have insufficient thermal and chemical resistance for this application.

1. Introduction

Environmental pollution deriving from diesel vehicle emissions is mainly due to the presence of large amounts of particulate matter consisting of particle clusters with a carbon core that adsorbs heavy hydrocarbons and metal oxides. Since the 1970s, diesel vehicles have been fitted with filters in order to minimize risks connected with particulate emission. Periodic regeneration by ignition of the particulate material trapped in the porous walls of the filter can lead to the release of a large amount of heat that may cause the temperature to rise suddenly to over 1000 °C [1].

The material currently used in the manufacture of diesel filters is highly porous cordierite ($Mg_2Al_4Si_5O_{18}$), which is favoured because of its low thermal expansion, good thermal shock resistance, chemical inertness, melt resistance and low cost. Unfortunately, the efficiency and durability of cordierite filters may be severely damaged by the following phenomena:

1. repeated severe thermal cycles, which lead to progressive filter degradation [2];
2. thermal stress due to local exothermic oxidative reactions during regeneration, which may generate cracks and fractures [1];
3. some pollutants adsorbed on the particulate material may react with cordierite, causing holes in the walls of the filter and alterations to the properties of the filter [3, 4].

These factors operate concurrently, reducing filter life expectancy.

The particulate material contains several oxides, such as those of sodium and lead (derived from accidentally contaminated fuel), vanadium (added as a catalyst to assist particulate combustion), iron (released by the engine), calcium and zinc (from lubricant oil). It has been proved [4, 5] that some of these oxides (particularly V_2O_5, PbO and Na_2O) react by solid state diffusion processes with cordierite (at 750, 550 and 500 °C, respectively).

It has also been observed [6] that Na_2O exhibits the most dangerous effect, followed by lead and vanadium oxides. The action of Na_2O is enhanced in the presence of vanadium pentoxide by synergy [5].

Several authors [7–9] and patents [10–18] propose alternative materials to cordierite for diesel filters, such as mullite, ZrO_2, TiO_2, α- or γ-Al_2O_3, SiC and Al_2TiO_5; but sillimanite (Al_2SiO_5), petalite [$LiAl(Si_2O_5)_2$], sialon (Si_3N_4), and BN have also been proposed.

Selection of a new filter material should take into consideration its economic and technological impact, but any alternative should have higher durability than cordierite. Silicon carbide is increasingly used for devices operating at high temperatures in combustion environments (heat exchangers, gas turbines, etc.) because of its good mechanical and thermal properties and oxidation characteristics [19]. These properties make SiC a potential candidate for use in the manufacture of diesel particulate filters [20–22].

In this paper, we aimed to determine the chemical resistance of SiC to Na_2O, PbO and V_2O_5 as a function of temperature. The starting reaction temperature, i.e. the lowest temperature at which structural and/or chemical changes were detected, was identified, as were the corrosion product phases that appeared.

2. Experimental procedure

2.1. Materials and procedure

Na_2CO_3 (as the source for Na_2O), PbO and V_2O_5 (all Aldrich + 99 % purity) and β-SiC powder (Lonza) were used. Interaction of SiC and single pollutants was investigated on samples of wet-milled mixtures of

0022–2461

silicon carbide and single oxide powders (ratio 1 : 1 by weight). This ratio was chosen to simulate the real conditions in use when local superficial contact between a pollutant particle and the filter wall takes place. After drying at 70 °C, a series of pellets ($\phi = 12.7$ mm) was obtained for each mixture by uniaxially pressing a weighed amount (200 mg) of powder at 400 MPa. Each compact was placed in a platinum crucible and heated to a selected maximum temperature (ranging from 400 to 1000 °C) in a programmable oven (Neztsch, heating rate: 10 °C min^{-1}, isotherm at final temperature for 5 min). After this treatment, each specimen was quenched to room temperature under vacuum in a desiccator. Samples were crushed to powder and studied by XRD and FT–i.r. analyses.

2.2. Analysis

FT–i.r. analyses were performed on KBr pellets using an Omnic system-controlled Nicolet Magna-IR 550 spectrometer in the spectral range 4000–250 cm^{-1}, with a resolution of 4 cm^{-1}. The spectra reported in the figures are in transmission and show only the more significant parts of the range. XRD powder patterns were obtained on an Inel XRG 3000 diffractometer with CoK_{α_1} radiation at an acquisition time of 30 min.

3. Results and discussion

Silicon carbide is inherently unstable in air and forms a thin SiO_2 layer in an oxidizing environment with high partial pressure of oxygen [23]. There is always an excess of oxygen, giving a high partial pressure, in diesel exhaust emissions. SiO_2 forms an effective reaction barrier because it has the lowest permeability to oxygen of any of the common oxides [24].

FT–i.r. analysis of as-received β-SiC powder (Fig. 1) shows the presence of amorphous SiO_2, the amount of which increases modestly after thermal treatment at 400, 700 or 900 °C. Bands from 1000 to 1300 cm^{-1} became sharper proving an initial crystallization of silica. The shifting of these bands, as well as the absorption at 465 cm^{-1}, suggests that rising temperature may be ascribed to an increase in the thickness of the SiO_2 film [25].

All reaction products formed by interaction of SiC and the oxides studied derive from reactions between the thin layer of SiO_2 and the oxides themselves.

3.1. Interaction with Na_2CO_3

The FT–i.r. spectra of sodium carbonate (a), silicon carbide (b) and their thermally untreated mixture (c) are presented in Fig. 2. The spectrum in Fig. 2a shows that sodium carbonate also contains the decahydrate form (typical single sharp bands at 1412, 902, 867, 687 cm^{-1} and large and broad shoulder between 1750 and 1600 cm^{-1}) [26]. It may be deduced from the spectrum in Fig. 2c that milling and drying the mixture reduce the amount of $Na_2CO_3.10H_2O$ in favour of Na_2CO_3. Fig. 3 illustrates sample FT–i.r. spectra when thermally untreated and after thermal

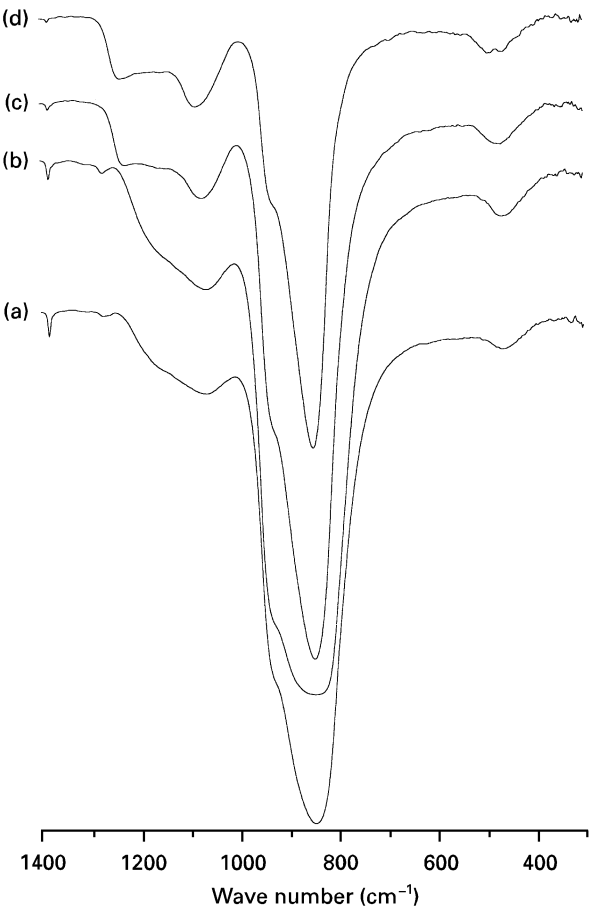

Figure 1 FT–i.r. spectra of as-received thermally untreated SiC powder (a) and after treatment at 400 °C (b), 700 °C (c) 900 °C (d).

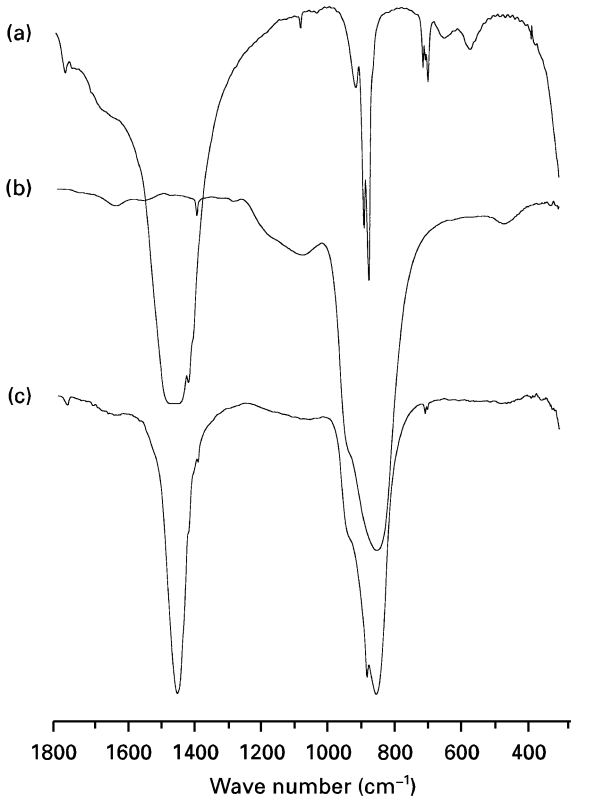

Figure 2 FT–i.r. spectra of Na_2CO_3 (a), SiC (b) and thermally untreated SiC–Na_2CO_3 mixture (50% by weight) (c).

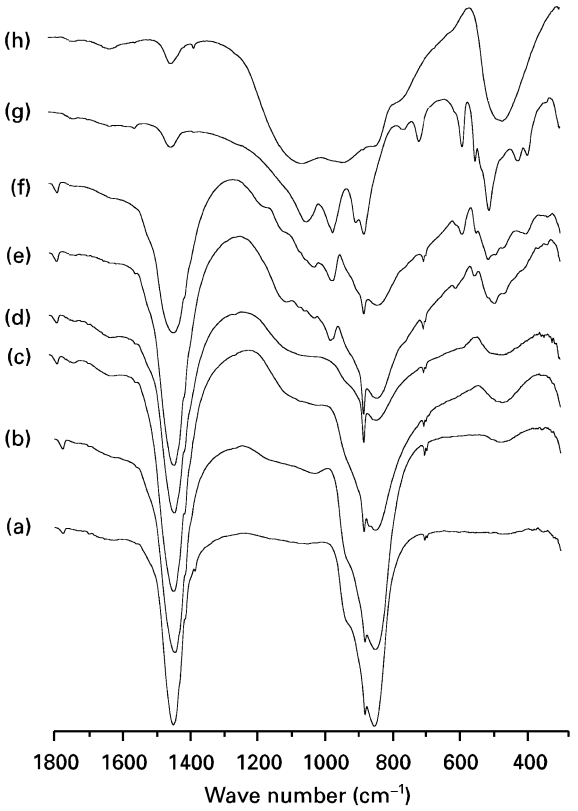

Figure 3 FT–i.r. spectra of a thermally untreated SiC–Na_2CO_3 mixture (50% by weight) (a) and after treatment at: 500 °C (b), 550 °C (c) 600 °C (d), 650 °C (e), 700 °C (f), 900 °C (g) and 1000 °C (h).

cycles at: 500, 550, 600, 650, 700, 900 and 1000 °C. Band assignment is presented in Table I. It may be observed that no changes occur until 500 °C (Fig. 3b). Broadening and lowering of the main SiC band (850 cm^{-1}) start at 550 °C (Fig. 3c) and are more evident at 600 °C (Fig. 3d), indicating that amorphization occurs.

New bands appear in the spectrum of the sample treated at 650 °C (Fig. 3e). These are mainly due to the formation of $Na_2Si_2O_5$ [27], as the XRD pattern confirms (Table II). The development of this phase and Na_2SiO_3 [27–28] is clearly shown in the i.r. spectrum of the sample treated at 700 °C (Fig. 3f) and confirmed by the corresponding XRD analysis. After treatment at 900 °C (Fig. 3g) the bands of Na_2SiO_3 become sharper and their intensities predominate over $Na_2Si_2O_5$. The XRD pattern is in agreement with FT–i.r., also showing an increased background signal. The spectrum of the sample heated at 1000 °C (Fig. 3h) corresponds to glassy $Na_2Si_2O_5$.

Jacobson [23, 29, 30] demonstrates that the protective SiO_2 layer on SiC is etched by various sodium salts (NaCl, Na_2SO_4, Na_2CO_3). The protective SiO_2 layer is dissolved by sodium carbonate. Oxygen then diffuses through Na_2CO_3 reacting with SiC to produce SiO_2, which immediately dissolves to form silicate. Dissolution can take place until all the Na_2CO_3 has been converted to sodium silicate.

The formation of $Na_2Si_2O_5$ observed at 650 °C may correspond to an initial diffusion step of Na^+ ions in the SiO_2 layer. The Na_2O–SiO_2 phase diagram shows that the most stable phases are sodium disilicate at

TABLE I Frequency assignments, ν (wave number, cm^{-1}), for FT–i.r. spectra of thermally treated Na_2CO_3–SiO_2 mixtures illustrated in Fig. 3

Thermal treatment temperature (°C)				Phase[b]	Explanation proposed[c]
650	700	900[a]	1000		
1444	1448	1452	1453	c	ν_{as} of CO_3^{-2} ions
	1180			d	
	1120			m	
1107				d	ν_{as} of SiO_4 groups with Si–O–Si bonds
1071	1071			S	
1055	1052	1049		d + m	
			1061	d[a]	ν_{as} of SiO_4 groups with Si–O–Si bands
1025	1027			d	ν_{as} of SiO_4 groups with Si–O^-Na^+ bonds
978	972	970		d + m	
			939	d[a]	ν_{as} of SiO_4 groups with Si–O^-Na^+ bonds
		901		m	ν_{as} of SiO_4 groups with Si–O^-Na bonds
880	880		881	c	δ_{op} of CO_3^{-2} ions
		877		m + c	ν_{as} of SiO_4 groups with Si–O^-Na bonds and δ_{oop} of CO_3^{-2} ions
842	840		845	SiC	ν_{as} of Si–C bonds
760	760	758		d	ν_s of SiO_4 groups with Si–O^-Na^+
			766	d[a]	ν_s of SiO_4 groups with Si–O^-Na^+
702	702			c	δ_{ip} of CO_3^{-2} ions
605	605			d	ν_s of SiO_4 groups with Si–O–Si bonds
		713		m	ν_{as} of SiO_4 groups with O–Si–O bonds
	587	585		m	ν_s of SiO_4 groups with Si–O–Si bonds
548	546	547		m	
509	510	506		d	δ of SiO_4 groups
489	490			S	
			469	d[a]	δ of SiO_4 groups

[a] Spectrum slightly broad.
[b] c = Na_2CO_3, d = $Na_2Si_2O_5$, d[a] = amorphous $Na_2Si_2O_5$, m = Na_2SiO_3, S = amorphous SiO_2.
[c] ν_{as} is asymmetric stretching; ν_s is symmetric stretching; δ_{op} is out of plane bending; δ_{ip} is in plane bending.

TABLE II XRD results: principal phases formed by reaction of SiC and Na_2CO_3 as function of temperature

Temperature (°C)						
500	550	600	650	700	900	1000
SiC(h)[a] Na_2CO_3(h)	SiC(h) Na_2CO_3(m)[b]	SiC(h) Na_2CO_3(m)	SiC(m) Na_2CO_3(m) $\beta Na_2Si_2O_5$(vl)[c]	SiC(m) Na_2CO_3(m) $\beta Na_2Si_2O_5$(l)[d] $\alpha Na_2Si_2O_5$(l) Na_2SiO_3(vl)	SiC(m) Na_2CO_3(l) $\beta Na_2Si_2O_5$(vl) $\alpha Na_2Si_2O_5$(vl) Na_2SiO_3(m)	SiC(h) Na_2CO_3(vl)

[a](h) = high.
[b](m) = medium.
[c](vl) = very low.
[d](l) = low.

low Na_2O content (at temperatures $< 789\,^{\circ}C$) and the biphasic $Na_2Si_2O_5$–Na_2SiO_3 system at a higher Na_2O concentration (at temperatures $< 837\,^{\circ}C$). The presence of sodium disilicate and metasilicate at 700 °C therefore suggests that the amount of sodium in the SiO_2 layer is higher than at 650 °C. Specimens treated at 900 and 1000 °C were attached to the bottom of the crucible, indicating the formation of liquid phases due to melts of carbonate (at a melting point of 851 °C) and disilicate (at a melting point of 874 °C). The latter should only partially be melted after treatment at 900 °C, because the sample was held at temperatures higher than the disilicate melting point only for few minutes. In fact, the FT–i.r. spectrum of this cooled sample shows just slightly diffuse bands. This is confirmed considering that after quenching this pellet was removed from the crucible easier than the one treated at 1000 °C, suggesting that the amount of liquid phase formed at 900 °C was lower than that formed at 1000 °C. The surfaces of these samples also showed the presence of pits and craters (at 900 °C these were less numerous than at 1000 °C), caused by gases, such as CO_2, liberated by the reaction of liquid sodium carbonate with SiO_2 [29]. In addition, according to Jacobson and Smialek [31], bubble formation derives from the direct attack of sodium silicate on unprotected SiC by a coupled oxidation–dissolution mechanism

$$SiC + 1.5O_2 \rightarrow SiO_2 + CO \quad (1)$$

$$(x-1)SiO_2 + Na_2SiO_3 \rightarrow Na_2O \cdot xSiO_2 \quad (2)$$

The occurrence of Reaction 2 at 1000 °C accounts for the presence of only glassy $Na_2O \cdot 2SiO_2$ in the FT–i.r. spectrum of this sample. In contrast at 900 °C, the prevalence of metasilicate, deriving from the easier diffusion of Na^+ ions in the liquid state, suggests that Reaction 2 is not significant at this temperature.

3.2. Interaction with V_2O_5

The spectra of SiC (a), V_2O_5 (b) and their thermally untreated mixture (c) are given in Fig. 4. The V_2O_5 spectrum (Fig. 4b) is in agreement with the literature [32]. Fig. 5 groups FT–i.r. spectra of the thermally untreated mixture (a) and of specimens after a thermal cycle at: 500, 550, 700, 750, 800, 900 and 1000 °C. On comparing these spectra, it may be seen that no changes occur until 500 °C (Fig. 5b) and, starting at 550 °C (Fig. 5c), only the increase in the amount of SiO_2 is observable (band at 1072 and broad shoulder at 1220 cm^{-1}) up to 700 °C (Fig. 5d).

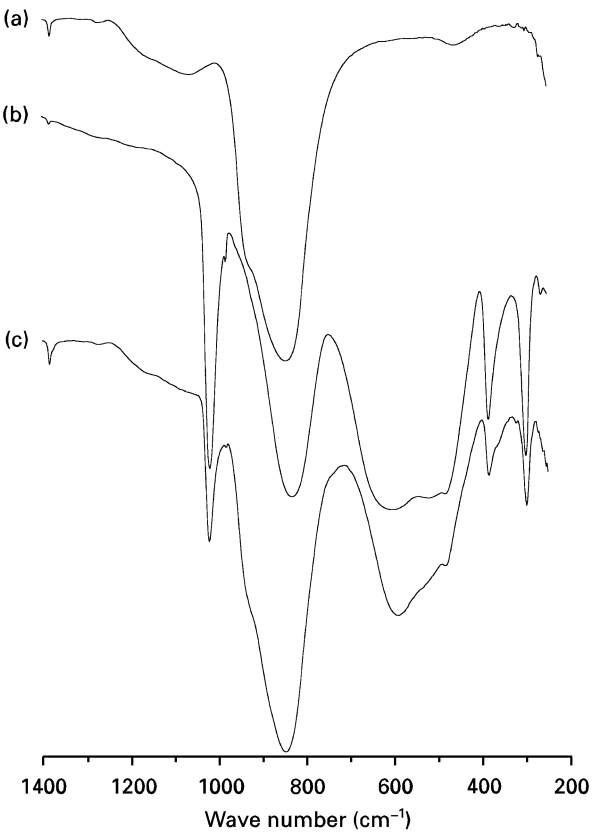

Figure 4 FT–i.r. spectra of SiC (a), V_2O_5 (b), and thermally untreated SiC–V_2O_5 mixture (50% by weight) (c).

V_2O_5 bands in the FT–i.r. spectrum of the sample treated at 750 °C (Fig. 5e) are broadened, shifted to lower wave numbers, and their intensities are reduced. Because the same changes can be observed after heating the pure oxide at this temperature, they can therefore be ascribed to the melting of the oxide. The lowering of vanadium absorptions in the 400–500 cm^{-1} region enables the silica band at 473 cm^{-1} to be seen. The XRD pattern (Table III) shows the appearance of monoclinic VO_2 [33] peaks and a considerable increase in background noise, which is also high at higher temperatures.

The FT–i.r. spectrum of a sample treated at 800 °C (Fig. 5f) resembles the one obtained at 750 °C (Fig. 5e) whereas XRD analysis shows more intense VO_2 peaks.

Over 900 °C (Fig. 5g, h), the absorption by ν_{as} of the V–O–V vibrations shifts to 820 cm^{-1} and prevails over SiC absorption. The other V_2O_5 bands again appear sharp. Both of these changes are observable in the FT–i.r. spectrum of the oxide alone after heating at the same temperature. The XRD pattern shows a reduced intensity of monoclinic VO_2 peaks at 900 °C, whereas at 1000 °C another modification of VO_2 [34] may be distinguished.

The mechanism of SiC corrosion in V_2O_5 melt has been investigated by Say *et al.* [35]. They proposed that V_2O_5, as a low melting point (658 °C) oxide, acts as a flux carrying a sufficient amount of oxygen from the air to the SiC–SiO_2 interface to enable Reaction 1. The hypothesis was supported by the observation that only SiO_2 formed as a silicate product (the solubility of silica in V_2O_5 melt is negligible) and considering bubble formation in the scale. These authors, however, noticed only a slight pitting attack after 2 h at 1000 °C. Using a shorter reaction time, we failed to observe any pitting phenomena in our specimens. The mechanism does not explain the reduction of V(V) to V(IV) observed at 750 °C, which is probably caused by the CO produced in the Reaction 1. In this regard, it should be borne in mind that the corrosion under vanadium pentoxide of silicon nitride, a non-oxide ceramic passivated by a SiO_2 layer like SiC, has been described as occurring by reduction of V(V)–V(III) [36].

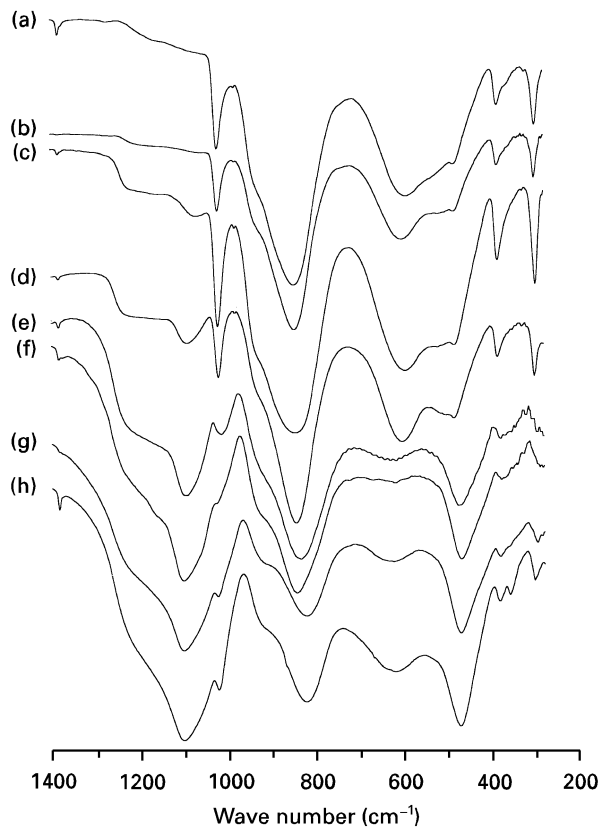

Figure 5 FT–i.r. spectra of thermally untreated SiC–V_2O_5 mixture (50% by weight) (a) and after treatment at: 500 °C (b), 550 ° (c), 700 °C (d), 750 °C (e), 800 °C (f), 900 °C (g) and 1000 °C (h).

3.3. Interaction with PbO

The spectra of single oxide powders and their thermally untreated mixture are given in Fig. 6. In the PbO spectrum of Fig. 6b, the band at 1420 cm^{-1} is due to lead carbonate [26] and the weak band at 353 cm^{-1} to PbO [37]. The spectrum in Fig. 6c is almost entirely the result of SiC absorption and the presence of PbO can be deduced from the band at 353 cm^{-1}. Fig. 7 shows the FT–i.r. spectra of samples treated at 500, 600, 650, 700, 900 and 1000 °C. The disappearance of the PbO band after heat treatment at 600 °C (Fig. 7c) is the first variation in the FT–i.r. spectra of this mixture. The corresponding XRD pattern shows increased background noise, lowered PbO peaks and the presence of Pb_2SiO_4 peaks. At 650 °C, the broad bands of the FT–i.r. spectrum (Fig. 7d) at 472 and 1050 cm^{-1} indicate the presence of a glassy silica phase. These bands and SiC absorption partially mask Pb_2SiO_4 bands that are distinguishable at 1080, 1020 and 670 cm^{-1} (Fig. 8). The glassy silica phase increases as the temperature rises up to 900 °C (Fig. 7f), when silica crystallizes to tridymite (bands at 1095, 793 and 472 cm^{-1}).

The amorphous nature of the sample treated at 650 °C is evident in the XRD patterns (Table IV), which show formation of Pb and the presence of Pb_2SiO_4 peaks. Above 700 °C, neither lead silicate nor oxide are detected any longer by XRD of the samples. Lead becomes the main phase and a well crystallized pattern is exhibited. XRD analysis of specimens

TABLE III XRD results: principal phases formed by the reaction of SiC and V_2O_5 as function of temperature

Temperature (°C)						
500	600	700	750	800	900	1000
SiC(m)[a] V_2O_5(h)[b]	SiC(m) V_2O_5(h)	SiC(m) V_2O_5(m)	SiC(m) V_2O_5(m) VO_2(l)[c]	SiC(m) V_2O_5(m) VO_2(m)	SiC(l) V_2O_5(m) VO_2(vl)[d]	SiC(l) V_2O_5(m) VO_2(vl)

[a](m) = medium.
[b](h) = high.
[c](l) = low.
[d](vl) = very low.

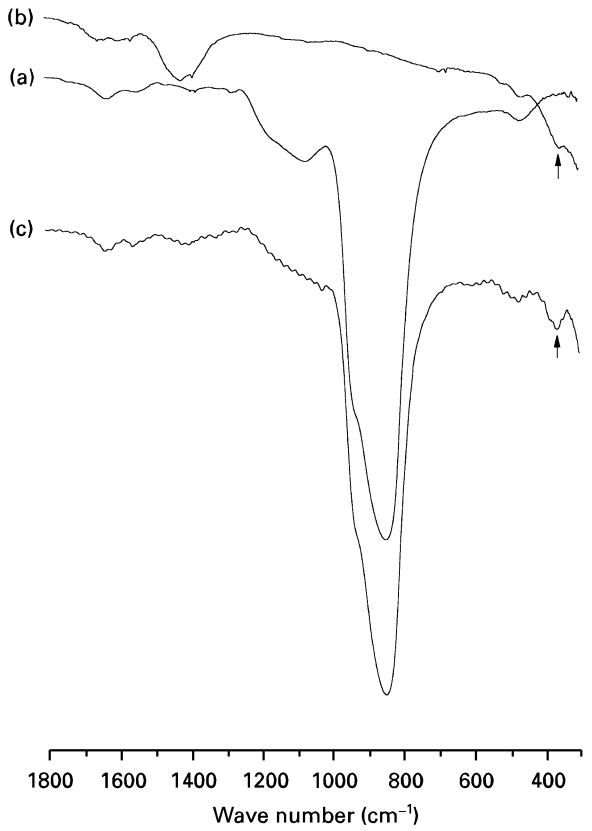

Figure 6 FT–i.r. spectra of SiC (a), PbO (b) and thermally untreated SiC–PbO mixture (50% by weight) (c). Arrows indicate the weak band at 353 cm^{-1} of PbO.

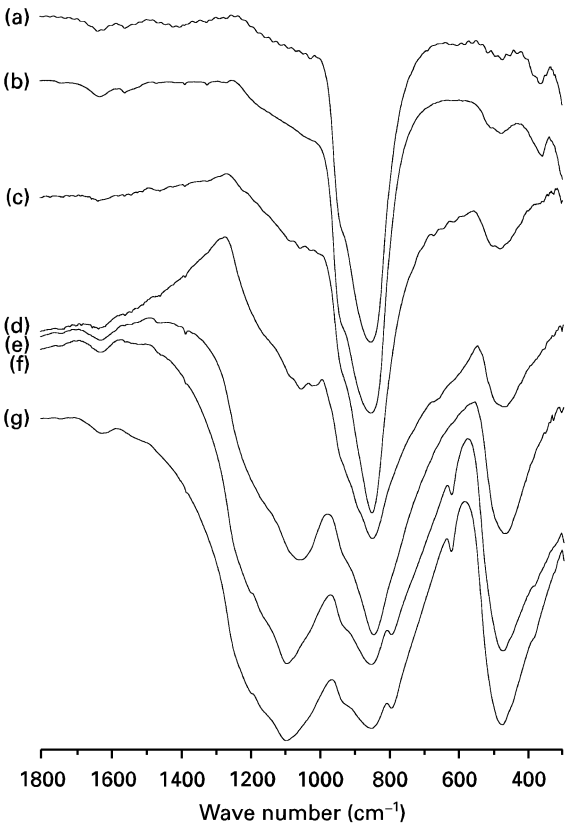

Figure 7 FT–i.r. spectra of thermally untreated SiC–PbO mixture (50% by weight) (a) and after treatment at: 500 °C (b), 600 °C (c), 650 °C (d), 700 °C (e), 900 °C (f) and 1000 °C (g).

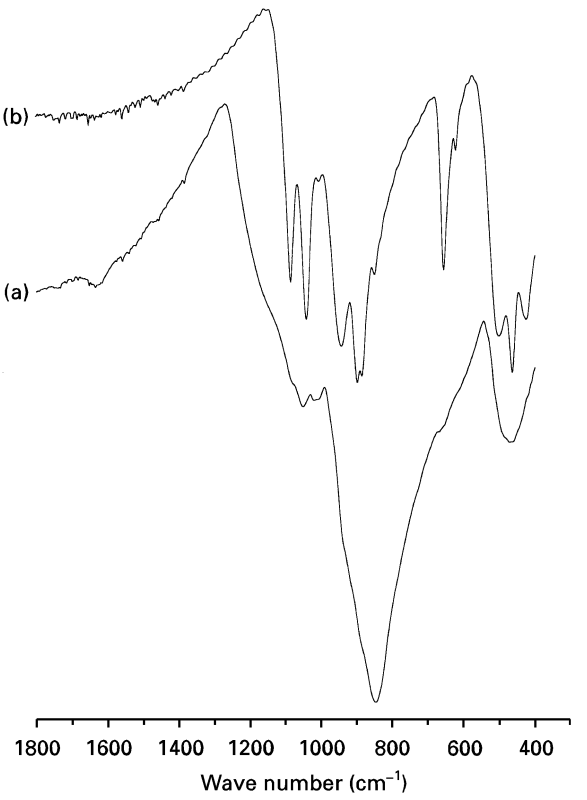

Figure 8 FT–i.r. spectra of SiC–PbO mixture after treatment at 650 °C (a) and well crystallized Pb_2SiO_4 (b).

heated at 900 and 1000 °C confirmed the formation of tridymite observed by FT–i.r.

To the best of our knowledge the interaction between SiC and PbO has not been addressed in the literature, while studies concerning glasses technology widely treat compounds between SiO_2 and PbO, but in the presence of stabilizing oxides (e.g. Al_2O_3, Na_2O, CaO). Based on the present results we suggest that a solid state reaction occurs between PbO and SiO_2 from 600 and 650 °C forming Pb_2SiO_4. Disappearance of Pb_2SiO_4 and PbO together with Pb formation, observed between 650 and 700 °C, suggest that lead silicate and oxide are reduced to lead by the reducing atmosphere of Reaction 1 [38–41].

4. Conclusions

The results on the interactions of SiC and single pollutant oxides have demonstrated that:

1. Sodium and lead oxides seem to be the most dangerous pollutants, because they start to react with the protective silica layer forming silicates at 550 and 600 °C, respectively.
2. Interaction with V_2O_5 begins at 750 °C and although it does not form new phases, it leads to accelerated SiC corrosion comprising an enhanced oxidation that produces a large amount of silica.
3. All oxides tested in this study affect silicon carbide at temperatures much lower than those reached by the filter during regeneration (< 1000 °C). Based on observations made in this study, interactions

TABLE IV XRD results: principal phases formed by the reaction of SiC and PbO as function of temperature

Temperature (°C)					
500	600	650	700	900	1000
SiC(l)[a] PbO(h)[b]	SiC(l) PbO(m)[c] Pb_2SiO_4(m)	SiC(l) PbO(l) Pb_2SiO_4(m) Pb(m)	SiC(l) Pb(h)	SiC(l) Pb(h) Tridymite(l)	SiC(l) Pb(h) Tridymite(m)

[a](l) = low.
[b](h) = high.
[c](m) = medium.

between SiC and contaminant oxides indicate potential problems using SiC as a diesel filter material.

References

1. A. GIACHELLO, P. P. DEMAESTRI, G. DE PORTU and S. GUICCIARDI, in Proceedings of CIMTEC, World Ceramic Congress, Montecatini, 24–30 June 1990.
2. S. MASCHIO, C. SCHIMID, E. LUCCHINI, S. ROITTI and A. GANDINI, Atti del Congresso Omaggio Scientifico a Renato Turriziani, Rome, 22–24 April 1992, Vol. II, pp. 2514–52.
3. A. NEGRO, L. MONTANARO, P. P. DEMAESTRI, A. GIACHELLO and A. BACHIORRINI, *J. Eur. Ceram. Soc.* **12** (1993) 493.
4. L. MONTANARO, A. BACHIORRINI and A. NEGRO, *ibid.* **13** (1994) 129.
5. L. MONTANARO and A. BACHIORRINI, *Ceram. Int.* **20** (1994) 169.
6. A. BACHIORRINI, *ibid.* **22** (1996) 73.
7. H. G. NITZSHE and H. KESSEL, *Haus Tech., Essen, Vortragsverooff* **206** (1969) 70.
8. R. D. BAGLEY, R. C. DOMAN, D. A. DUKE and R. N. MCNALLY, SAE Technology Paper No. 730 274 (SAE, Warrendale, PA, 1973) 7pp.
9. I. M. KOLESNIKOV and I. N. FROLOVA, *Zh. Prikl. Khim.* (*Leningrad*) **55** (1982) 561.
10. F. J. SERGEYS, *US Patent* 3 926 851, December (1975).
11. Y. TAKENCHI, *German patent* 2 411 222 August (1976).
12. J. NEMETH, *US Patent* 4 040 998 August (1997).
13. T. NAKAMURA, *Jpn Tokyo Koho JP Patent* 78 121 010 October (1978).
14. K. NISHIMOTO, N. YOKOYAMA, T. SERA and M. SUWA, *ibid. Jpn Tokyo Koho JP Patent* 78 138 992 December (1978).
15. MATSUSHITA ELECTRIC INDUSTRIAL CO. LTD, *ibid. Koho JP* 58 124 544 July (1983).
16. *Idem*, *ibid.* August (1983).
17. Y. ONO, A. NISHINO, Y. TAKEUCHI and H. NUMAMOTO, *ibid.* November (1985).
18. B. K. SPERONELLLO, *European Patent R* Appl. EP187007 (Cl C04B38/04), 9 July (1986) US Patent Appl. 682 004, 14 December (1984).
19. E. M. LENOE, R. N. KATZ and J. J. BURKE (eds), "Ceramics for high performance applications III" (Plenum, NJ, 1983).
20. M. MONTORSI, C. BADINI and E. VERNÈ, *Ceramurgia* **2** (1994) 41.
21. A. ITOH, K. SHIMATO, T. KOMORI, H. OKAZOE, T. YAMADA, K. NIIMURA and Y. WATANABE, SAE Paper No. 930 360 (SAE, Warrendale, PA, 1993) pp 111–9.
22. H. OKAZOE, T. YAMADA, K. NIIMURA, Y. WATANABE, A. ITOH, K. SHIMATO and T. KOMORI, *ibid.* No. 930 361 (SAE, Warrendale, PA, 1993) pp. 121–8.
23. N. S. JACOBSON, *J. Amer. Ceram. Soc.* **76** (1993) 3.
24. N. J. SHAW *et al.* NASA Report No. TM-100169 (NASA Lewis Research Centre, Cleveland, OH, 1987).
25. A. KUCIRRKOVA and K. NAVRATIL, *Appl. Spectrosc.* **48** (1994) 113.
26. V. C. FARMER, 'The infrared spectra of minerals" (Mineralogical Society, London, 1974) pp. 227–79.
27. A. BACHIORRINI and G. ABBIATI, *Ceramurgia* **3** (1983) 97.
28. A. N. LAZAREV and T. F. TENISCHEVA, *Opt. and Spectrosc.* **9** (1960) 37.
29. N. S. JACOBSON, *J. Amer. Ceram. Soc.* **69** (1986) 74.
30. N. S. JACOBSON and J. L. SMIALEK, *ibid.* **68** (1985) 432.
31. *Idem*, *J. Electrochem. Soc.* **133** (1986) 2615.
32. L. ABELLO, E. HUSSON, Y. REPELIN and G. LUCAZEAU, *Spectrochim. Acta* **39A** (1983) 641.
33. Powder diffraction file, card 9-142 (Joint Committee on Powder Diffraction Standards, Swarthmore, PA, 1961).
34. *Idem*, card 31-1438.
35. W. E. SAY, J. K. WU and W. L. CHEN, *J. Mater. Sci.* **25** (1990) 1614.
36. T. SATO, S. TERAUCHI, T. ENDO and M. SHIMADA, *ibid.* **25** (1990) 1231.
37. D. M. ADAMS and D. C. STEVENS, *J. Chem. Soc. Dalton* **11** (1977) 1096.
38. R. W. RUSSEL and P. C. HAYES, *Symp. Series: Australas. Inst. Min. Metall.* **51** (1987) 167.
39. M. M. HUSSAIN and D. R. MORRIS, *J. Metals* **8** (1985).
40. *Idem*, *Metall. Trans. B* **17** (1986) 575.
41. I. R. POLYVYANNYI and V. P. OVCHARENKO, "Kinetics of the reduction of lead from crystalline lead–calcium silicates by hydrogen", *Institute Metallurgical Obogashch.* (Alma-Ata, USSR), *Deposited Document* (1983) VINITI pp. 1172–83.

Received 19 July 1996
and accepted 8 July 1997